Chinese Science Bulletin

The seasonal cycle of interhemispheric oscillations in mass field of the global atmosphere

LU ChuHan[1], GUAN ZhaoYong[1†], MEI ShiLong[1,2] & QIN YuJing[1]

[1] Key Laboratory of Meteorological Disaster (KLME) and College of Atmospheric Sciences, Nanjing University of Information Science and Technology, Nanjing 210044, China;
[2] The Meteorological Observatory of Jiaxing Meteorological Bureau, Jiaxing 314000, China

Using the daily and monthly data of surface air pressure, meridional wind, radiation and water vapor from NCEP/NCAR reanalysis for the period of 1979—2006, we have examined the seasonal variations of the interhemispheric oscillations (IHO) in mass field of the global atmosphere. Our results have demonstrated that IHO as observed in surface air pressure field shows the distinct seasonal cycle. This seasonal cycle has an interhemispheric seesaw structure with comparable annual ranges of surface air pressure in the Southern and Northern Hemispheres. Mass of water vapor changes out-of-phase between the Southern and Northern Hemispheres, showing clearly a seasonal cycle with its annual range almost equivalent to annual range of the IHO seasonal cycle. Amazingly, the cross-equatorial flow is found to be induced by annual changes in water vapor mass as a response of the atmosphere to seasonal cycle of forcing from hemispheric net surface short- and long-wave radiations. The IHO seasonality exhibits its larger variations in magnitude in mid-latitudes other than in other regions of the globe. Additionally, our results also show that the global air mass is redistributed seasonally not only between the Northern and Southern Hemispheres but also between land and sea. This land-sea air mass redistribution induces a zonal pattern of surface air pressure in the Northern Hemisphere but the meridional pattern in the Southern Hemisphere.

interhemispheric oscillation, atmospheric mass, seasonal cycle, cross-equatorial flow of air mass

Surface air pressure (SAP) is one of the most important parameters describing climate change[1]. The evolutions of SAP are indicative of atmospheric mass (AM) distributions and the atmospheric circulation variations. Usually, AM is assumed to be conservative in numerical simulations using atmospheric general circulation models[2−4]. Therefore, the SAP is a very sensitive and useful parameter[5] in evaluating numerical models. In 1981, Trenberth, by analyzing the air pressure at both surface and sea level, discovered that, due to the seasonal variation of vapor mass in the atmosphere, global surface pressure experiences an annual cycle ranging from 984.47—984.97 hPa, maximizing in August[2]. The mean surface air pressure over a hemisphere is found to be higher in winter but lower in summer. This phenomenon has also been detected by earth's deformation research[3]. Based on a range of global gridded reanalysis data available, including, for example, NCEP, ERA and JRA, numerous researchers investigated the change in AM globally and hemispherically from surface air pressures and water vapor pressures, acquiring the seasonal cycle of AM as a strong signal of climate variation[4−7]. However, atmospheric activities are not confined just to the hemisphere but cross the equator for the interhemispheric exchange of air mass, momentum and energy, thereby linking up the atmosphere of both the

Received January 28, 2008; accepted June 2, 2008; published online August 27, 2008
doi: 10.1007/s11434-008-0316-3
†Corresponding author (email: guanzy@nuist.edu.cn)
Surpported by the National Natural Science Foundation of China (Grant No. 40675025), the Project of National Key Basic Research Development (Grant No. 2004CB418302) and the Key Lab of Meteorological Disasters (KLME) of Nanjing University of Information Science and Technology (NUIST) (Grant No. KLME060101)

hemispheres[4,7,8]. Besides, there is a sort of linkage in the sea ice cover between bi-hemespheric polar regions[9]. As demonstrated in Guan and Yamagata[10], the interannual anomalies of AM in both hemispheres show a seesaw pattern, thereby proposing the concept of interhemispheric oscillation (IHO), together with the interannual distribution of monthly IHO and its evolution presented. Their study did not involve the interannual variation of IHO in specific season and seasonality, however.

Seasonal change in position of the thermal equator on the earth leads to bi-hemispheric AM transport in summer opposite to winter, resulting in IHO seasonal change, which begets the redistribution of the atmosphere on a global basis, including its composition, e.g., ozone, greenhouse gases and pollutants. Moreover, the surface pressure fields determine, to great extent, near-surface wind fields[11], such that the IHO seasonal variation is bound to bear a close relation to monsoons. Using 1979—2006 NCEP/NCAR reanalysis, the authors make an attempt in the present article to explore the IHO seasonal change to address the distribution and seasonal difference in AM on a hemispheric scale in conjunction with the study of main internal factors for IHO seasonal variation consisting of hemispheric water vapor mass and cross-equatorial air mass flow, as well as forcing factors, e.g., surface radiations, all of which experience seasonal change. Eventually, seasonal IHO-caused global AM space pattern is addressed.

1 Data

Data used in the present article are from NCEP/NCAR reanalysis sets[12], with the variables including daily mean surface air pressure (P_s), net surface short-/long-wave radiation, atmospheric precipitable water (P_w), monthly mean surface air pressure, precipitation rate (P), evaporation rate (E), surface (V_s) and upper-air winds (V) at 2.5°×2.5° resolution for January 1, 1979—December 31, 2006. Besides, JRA25[13] and ERA40[14] datasets are employed to validate the results from NCEP/NCAR data. The CAM3[15] and FrAM1.0[16] simulations are utilized to prove the existence of the IHO seasonal cycle.

2 Seasonal evolution pattern of IHO

The seasonal IHO displays a seesaw pattern of bi-hemispheric AM. Following Trenberth and Guillemot[17], global AM total can be calculated by means of the expression for surface pressure in the form:

$$m = \frac{2\pi a^2 f_D}{g_0} \int_{-\pi/2}^{\pi/2} p_s(\phi)\cos\phi \mathrm{d}\phi , \quad (1)$$

where f_D (= 1.0020) denotes the parameter of earth's deformation, and ϕ the latitude. From (1) we can derive the formula for hemispheric AM,

$$m_H = \frac{2\pi a^2 f_D}{g_0} \int_0^{\pi/2} p_s(\phi)\cos\phi \mathrm{d}\phi . \quad (2)$$

Undoubtedly, the use of SLP (sea surface pressure) on a weather map for estimating northern AM and its variation had limitations, as shown in early studies, whose data were sparse in some oceanic regions on the globe and of lower reliability (compared to those gleaned today), leading to greater bias as regards hemispheric AM transfer[18]. We calculated 1979—2006 daily pressure P using eq. (2) as the total AM of the Southern and Northern Hemispheres (Figure 1(a), (b)), indicating that the seasonal change takes mainly one-wave form that is opposite in phase for both hemispheres, with maximum of yearly change about 2×10^{15} kg, exhibiting remarkable IHO features. The northern AM maximizes in winter (DJF) and minimizes in summer (JJA), the valley being clearer in July—August and the peak is maintained almost half a year (December—April). The reversal happens in the austral hemisphere. The inhomogeneity of diabatic heating between the hemispheres leads to atmospheric pressure (mass) lower in the warm than in the cold hemisphere, in conformity with 'thermal theory of pressure change'[19]. Additionally, the southern AM is significantly higher as compared to the northern AM[7]. The greatest monthly difference of AM between the hemispheres reaches 18×10^{15} kg, which is due to the fact that both the mean surface temperature and elevation are lower in the Southern Hemisphere (with the difference of averaged evaluation by 92 m and difference of long-term mean July surface temperature by 10.8℃ between the Southern Hemisphere and the Northern Hemisphere) in comparison to the northern counterparts, responsible for AM higher in the austral than boreal hemisphere. It deserves attention that the seasonal change in the hemispheric AM of 4×10^{15} kg is equivalent to the variation of hemispherical mean P_s reaching 2 hPa. From the geostrophic wind relation ($u_g = -\Delta p/(f\rho\Delta y)$), where Δy denotes the difference in distance between latitudes at

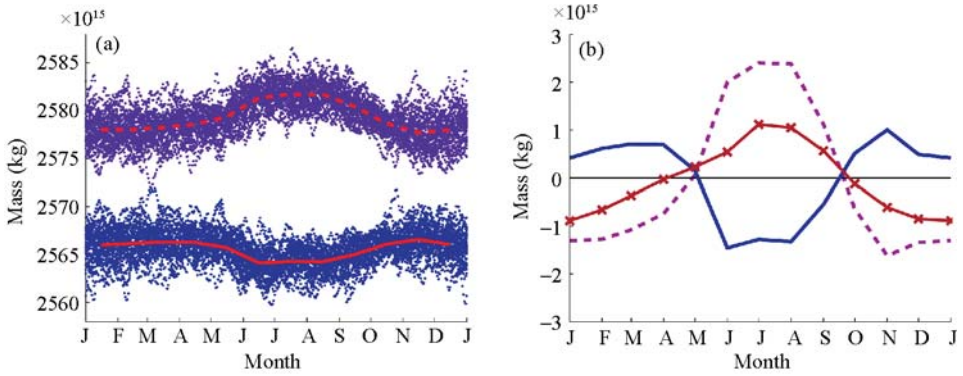

Figure 1 (a) The 1979—2006 daily atmospheric mass in purple (blue) for the Southern (Northern) Hemisphere, with the inside dashed (full) line denoting multi-year monthly means; (b) the monthly climate means for the austral, boreal and globe designated by dashed, solid, and crossed line, respectively, where related yearly mean is subtracted.

which zonal mean P_s peak and its valley are located for each hemisphere, with $\pi/4$ as the reference latitude, the change at $u = 0.35$ m s^{-1} in zonal wind can be produced approximately so that the meridional distribution of AM anomalies is able to affect zonal basic flow.

3 Internal factors governing seasonal variations of atmospheric mass IHO

The hemispheric AM change involves its variation inside the hemisphere and interhemispheric transmission. The internal factors include dry air and vapor mass but no evidence has been found hitherto about sources/sinks strong enough to change dry air mass on a hemispheric basis in the IHO seasonal variation. As a result, vapor mass and cross-equatorial mass flows are the internal ingredients of much importance to the AM IHO seasonal variation, which are dealt with for their own seasonal variations and interrelations to IHO.

3.1 Water vapor mass

Vapor acts as an important component of AM seasonal variation and also a principal gas absorbing solar short- and surface long-wave radiation, its content being associated with the thermal condition of the surface and air, thereby affecting the AM IHO directly and indirectly. To investigate the relative importance of vapor in IHO seasonal variation, we calculate the water vapor pressure (P_w) in the atmosphere, which is expressed, with reference to Chen et al.[4], as

$$p_w = \int_0^{p_s} q\mathrm{d}p = gw, \tag{3}$$

where w designates the precipitable water throughout the atmosphere. By use of eqs. (1)—(3) we have the expressions for global (mw) and hemispheric (mw_H) vapor mass, viz.,

$$\begin{cases} mw = \dfrac{2\pi a^2 f_D}{g_0}\displaystyle\int_{-\pi/2}^{\pi/2} p_w(\phi)\cos\phi\mathrm{d}\phi, \\ mw_H = \dfrac{2\pi a^2 f_D}{g_0}\displaystyle\int_{0}^{\pi/2} p_w(\phi)\cos\phi\mathrm{d}\phi. \end{cases} \tag{4}$$

Figure 2(a) (2(b)) delineates the change in multiyear daily vapor mass (monthly mean mass of vapor and dry air) for each of the hemispheres. Compared with Figure 1, we see that the annual change of vapor mass in each of the two hemispheres amounts to 3×10^{15} kg, which is slightly smaller than that of seasonal changes of AM (Figures 1(b) vs 2(b)). The annual cycle of water vapor mass and that of AM in a hemisphere are out of phase with phase difference of six months, which indicates that the seasonal variation of vapor mass is the main component of AM seasonal IHO. As compared to the changes of both the wet air atmosphere and water vapor, the dry air mass changes in out of phase between the two hemispheres to even greater extent, reaching the range over of 7×10^{15} kg from its minimum to maximum values (Figure 2(b)). Note that the increase of water vapor (its molecular weight being 18) in the atmosphere implies the decrease of the air density. The increase of water vapor in the atmosphere in one hemisphere begets the transfer of dry air mass into another hemisphere through cross-equatorial flows. The peak of seasonal variation in water vapor (P_w) averaged over the Northern Hemisphere is larger than that in the Southern Hemisphere, in association with the annual mean thermal equator inclined towards the Northern Hemisphere, whose land area is bigger, such that the solar radiation heating is stronger over the land as compared to waters. From the

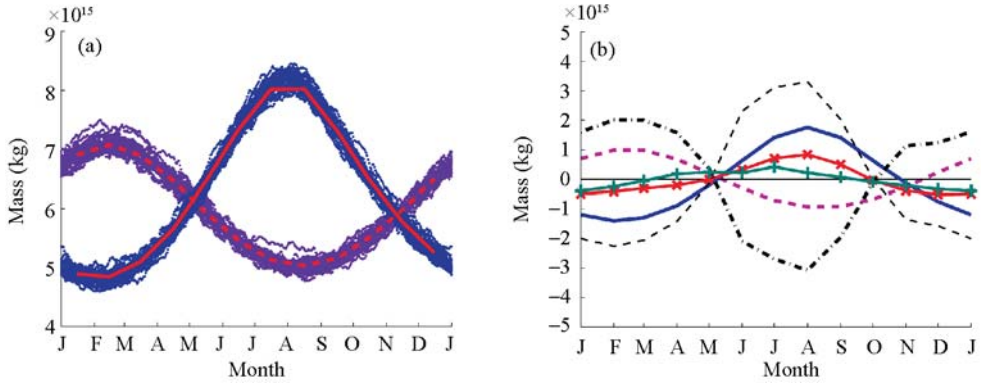

Figure 2 (a) The 1979—2006 daily vapor mass in purple (blue) for the Southern (Northern) Hemisphere, with long-term monthly mean given inside by dashed (solid) line; (b) 1979—2006 monthly vapor mass total (as climate values) designated by dashed (full) line for the Southern (Northern) Hemisphere, and the dry air mass total by thin dashed (dotted-dashed) line for the Southern (Northern) Hemisphere, while the mean over global vapor mass (dry air mass) is marked by the line with crosses (pluses) upon, with its yearly average removed.

Clausius-Clapeyron equation we know that warm (cold) air accompanying low (high) systems at surface is liable for still higher (lower) vapor content in the air, causing vapor to run from the winter into the summer hemisphere[20] by dint of low-level cross-equatorial flows, responsible for more vapor in boreal hemisphere in summer than in the austral hemisphere. Because of the dominance of vapor transport from the Southern Hemisphere on a yearly mean basis[20], the northern vapor mass is higher by 2.5×10^{14} kg despite the vast expanse of water available in the Southern Hemisphere.

The global mean dry air mass experiences little variation whilst global mean AM and vapor mass have their changes in phase with similar annual ranges about 0.8×10^{15} kg from their minimum to maximum values (Figures 1(b) vs 2(b)), indicating the seasonal variation of global AM relating predominantly to the component of vapor mass and demonstrating the basic conservation of dry air mass globally in its seasonal variation[2,4,6,21]. Problems as to hemispheric vapor mass change including its local component change and vapor transfer from the other hemisphere will be addressed in the following.

3.2 Cross-equatorial mass flow

The equator is the geographic division between the hemispheres and also the latitude for opposite signs of the Coriolis parameter on both sides. The interhemispheric AM exchange is answerable for its redistribution of global AM over the hemispheres, leading to the change in surface air pressure on a hemispheric basis to cause the AM IHO seasonal cycle. In accordance with the mass conservation principle, assuming the seasonal variation of other gaseous constituents inside the hemisphere to be relatively small, i.e., hemispheric total dry air mass sources/sinks caused total dry air mass to undergo insignificant variation, the monthly change in the hemispheric AM (Δm) can be given by

$$\Delta m = E - P + I_1 ,$$

in which E signifies the monthly evaporation (E), P the monthly precipitation, with their difference denoting the variation in monthly vapor mass in the hemisphere, and I_1 the monthly cross-equatorial mass flow, consisting of dry air and vapor. Therefrom, we get I_1 in the form:

$$I_1 = \Delta m - (E - P) . \quad (5)$$

In line with eq. (5) it is evident that I_1 obtained for either of the hemispheres with the same procedure leads to the identical results. Here we present Δm and $E - P$ as well as I_1 calculated thereby for the Northern Hemisphere (Figure 3(a), (b)). Figure 3(a) shows that the monthly variation in boreal AM (Δm) exhibits explicit IHO out of phase for both the hemispheres, with the annual changes (2.5×10^{14} kg) about half of the annual changes of AM IHO (m). In addition, the change in sign of AM for each of the two hemispheres occurs in January and June, indicating AM to steadily increase (decrease) in summer to autumn (winter to spring) for the Northern Hemisphere and v.v. for the Southern Hemisphere, in good correspondence to m curve of Figure 1.

The hemispheric vapor mass change calculated by $E - P$ (Figure 3(b)) shows that, on the whole, the E–P changes in a very different manner to Δm of the Northern Hemisphere. When the Δm reaches its minimum around April (Figure 3(a)), magnitude of $E - P$ is around zero. However, when $E - P$ reaches its maximum in boreal summer (Figure 3(b), solid curve), the total atmospheric mass changes little, as displayed by the Δm with its value close to zero (Figure 3(a), solid curve). $E - P$

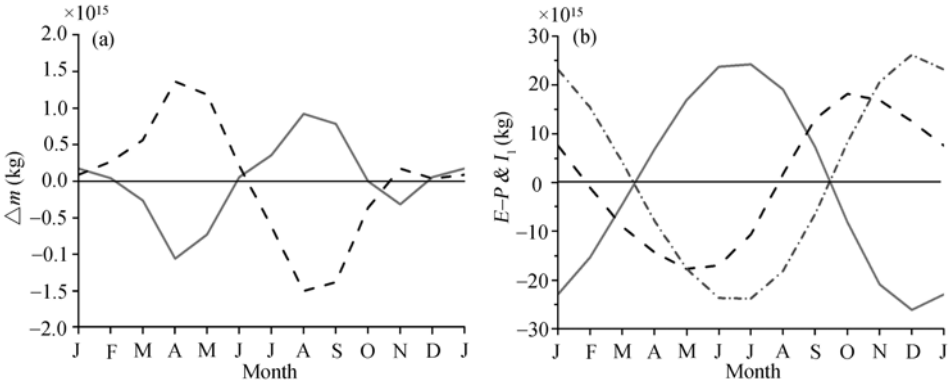

Figure 3 (a) Multi-year mean atmospheric mass variation Δm for the Northern (solid) and Southern Hemisphere (dashed line); (b) $E - P$ (solid for the Northern Hemisphere whereas dashed for Southern Hemisphere) and I_1 (dotted-dashed).

curve in Figure 3(b) exhibits a one-wave pattern, with the magnitude larger by one order than Δm value. Seasonal variation of I_1 has an out-of-phase relation with the variation of $E - P$ of the Northern Hemisphere, with the annual changes in values comparable to each other. These results indicate that (1) on a seasonal basis, hemispheric AM changes in close relation to vapor content; (2) interhemispheric mass exchange is another significant component of the change in hemispheric AM, and spring and autumn serve as active seasons for interhemispheric AM exchange[4,22]. The I_1 as computed from Δm and $E - P$ is comparable to $E - P$ in the order of magnitude, indicating that hemispheric evaporation and precipitation lead to the production of the net transport of cross-equatorial AM. That arises due to H_2O molecular weight being 18; the augmentation (reduction) of vapor mass is associated with the decrease (increase) of air density in the hemisphere, thereby forcing air mass to go into another hemisphere to generate cross-equatorial mass flows, by which to realize interhemispheric AM exchange. This mechanism differs pronouncedly from that associated with thermal driving proposed by early researchers[18]. Of course, I_1 contains both the component brought by vapor change and the component of cross-equatorial flow happening due to air column expansion (contraction) owing to heating (cooling) in differing months of one (the other) hemispheric atmosphere, the contraction seeming a lot smaller compared to the expansion.

4 Seasonal variation in solar radiation

Solar radiation is the direct driving factor for AM transfer. Its seasonal variation makes for inhomogeneous heating between the hemispheres, affecting the interactions between the bi-hemispheric atmospheres (including the seasonal change in atmospheric circulations and cross-equatorial flows[23] as well as in the total vapor mass). Consequently, solar radiation is the main external factor for AM IHO seasonal variation. As early as the 1950s, Chinese scientist Yang[18] concluded that solar radiation when heating a hemisphere is responsible for interhemispheric AM transfer in his study of SLP-calculated northern AM and his computing interhemispheric exchange. Figure 4 depicts the monthly net surface short- and long-wave radiation for both the hemispheres (with the net radiation referring to the difference between incoming and outgoing values). Figure 4(a) clearly shows that the solar radiation is strong in summer and weak in winter for the Northern Hemisphere in phase with vapor pressure change (Figure 2), suggesting an important role played by net surface short-wave radiation in water evaporation. The annual range and peak value of northern mean net surface short- wave radiation are marginally smaller than the southern equivalents, in association with the higher mean content of vapor in the northern atmosphere, which acts as the principal ingredient absorbing the radiation.

On the other hand, long-wave radiation represents the chief source of atmospheric energy. The atmosphere is liable to the radiative heating (cooling) for its expansion (contraction), leading to AM transmission. Figure 4(b) gives the variation in net long-wave radiation at surface on a hemispheric scale, indicative of its variation broadly related to that of Δm, suggesting that long-wave radiation heating in spring is the strongest in the boreal hemisphere, driving its atmosphere to migrate southward, crossing the equator, resulting in the biggest negative Δm, and v.v. in autumn.

The seasonal variation in mean temperature relative to hemispheric air density and subjected to areal weigh-

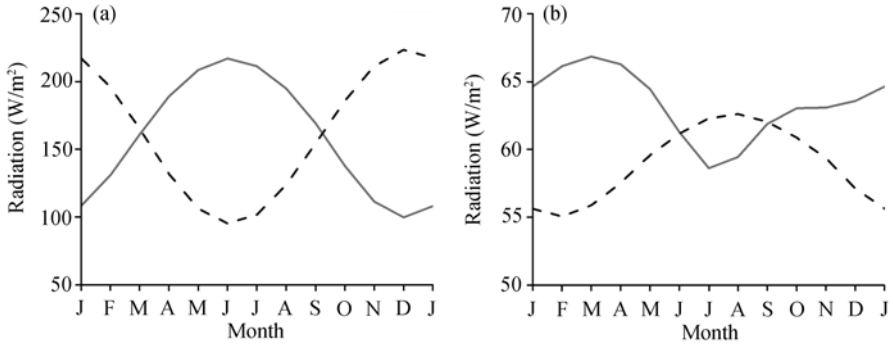

Figure 4 (a) The net surface short-wave radiation averaged hemispherically over 1979—2006 for the austral and boreal hemispheres; (b) same as in (a) but for long-wave radiation.

ing is an indicator of the change in solar heating. The calculations presented here (figure not shown) suggest that the hemispheric mean temperature (the annual mean being removed) reaches its maximum (minimum) in summer (winter), with boreal (austral) annual change amount about 8 K (5 K). On the other hand, corresponding to the change of hemispheric atmospheric mass (Δm), change of the northern (southern) mean temperature exhibits its maximum (minimum) in spring (autumn), with the annual change amount over 4 K (2 K). The change in hemispheric mean air column height (40—60 geopotential meters, when considered in a static manner) caused by change in hemispherically averaged temperature leads to the modification of pressure gradient force between the hemispheres, and despite the wind-field made to adjust itself toward the pressure field, interhemispheric AM transfer remains possible.

5 Difference in AM distribution between winter and summer

The seasonal shift of the heat equator in position leads to interhemispheric AM transfer in the opposite direction in winter and summer, thereby causing AM and its constituents to be redistributed globally. Shown in Figure 5(a) and (b) are the vertical structures of zonally averaged geopotential heights (h) on a hemispheric scale in winter and summer, indicating h having noticeable IHO, with its high-valued zones located largely at extratropics. In boreal summer the atmosphere gets heated, leading to the 4 K rise in temperature for all the isobaric surfaces and in association with the heating, vapor content in the column is increased, air density reduces and the column is stretched with the consequence that the geopotential height rises by more than 10 gpm for each isobaric surface, in sharp contrast to the summer (cold) conditions of the austral hemisphere, only with the change range a bit smaller compared to that in boreal summer. Additionally, northern h high-values cover a wider region and deeper vertically in comparison with the southern equivalents, possibly in relation to the land-sea contrast between both the hemispheres.

To visualize the seasonal AM difference, the 1979—2006 mean P_s distributions for winter (DJF) and summer (JJA) are presented in Figure 5(c), (d) and (e), where subtracted from a P_s value is the yearly mean for the related gridpoint because the unprocessed P_s climate map is able to reflect the topographic features alone[24]. Two salient features can be found in Figures 5(c) and (d). (1) North of 15°N, AM distributions in winter and summer are marked by remarkable land-sea contrast, with wintertime positive anomalies mainly over Asia (with exclusion of the Tibetan Plateau[25]), central-eastern North America, Chinese Changjiang-Huaihe river valley and North China in conjunction with the negative anomalies that reside in the central Pacific and the Atlantic, north of 30°N, in association with AM transported from the oceans to the landmass[18], and *vice versa* in the summer, in which zonal AM distributions differ greatly, displayed as a seesaw with ~20 hPa amplitude in the zonal direction, whereof the oscillation that is similar to the mid-latitude Asian-North Pacific teleconnection (APO) is especially significant[26]. The season-dependent changes in the orientation and magnitude of temperature gradients on account of land-sea thermal contrast are responsible for the genesis and altered intensity of Asian-Australian summer monsoon[23], and Asian subtropical monsoon[27], for example; (2) distributed over tropics and austral extratropics are chiefly banded AM positive and negative anomalies, with a me-

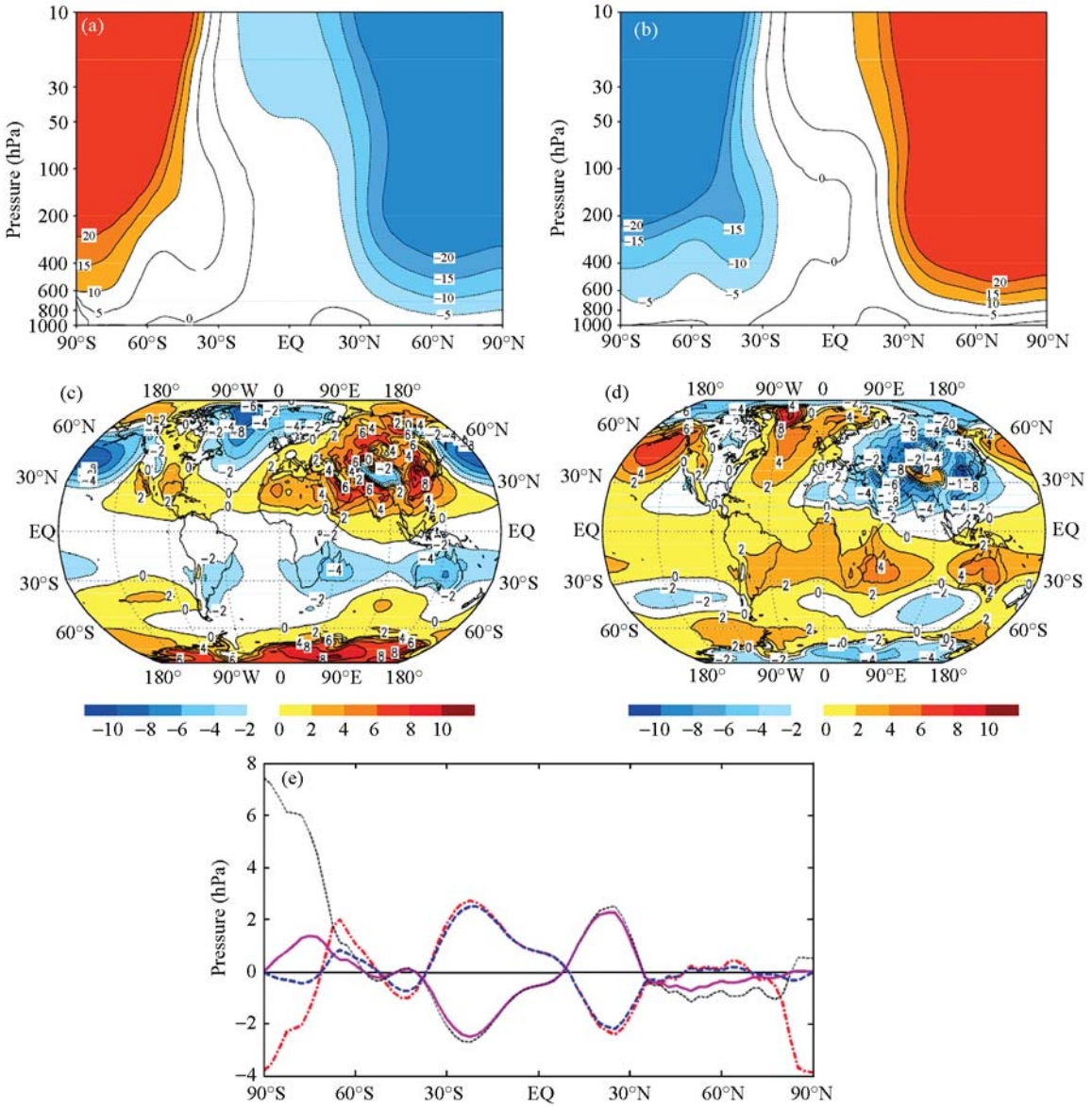

Figure 5 1979−2006 climatological geopotential heights (gph) in winter (DJF (a)), and summer (JJA (b)), P_s in winter and summer (c) and (d), seasonally anomalous P_s averaged zonally (e) (with gph and P_s being values arising from the subtraction of multi-year means). The interval of contours is 5 gpm in (a) and (b) and of 2 hPa in (c) and (d); the thin dashed (dot-dashed) line in (e)) denotes winter (summer) for DJF (JJA) where solid (dashed) line represents the areally weighed P_s in winter (summer), with the legend given below (c) and (d). The ordinate coordinate designates hPa.

ridional pattern of AM as the predominant type. Low (high) pressure systems are related to warm (cold) surface, and the surface diabatic effects are noticeable enough to be the principal cause of AM anomalous distribution[28]. Corresponding to Figure 5(c) and (d), Figure 5(e) displays a seesaw of zonally averaged anomalous AM that evolves as a function of latitude between winter and summer with greater amplitudes at subtropics and bi-hemispheric polar regions, indicating that the winter and summer abnormal AM emerges mainly at those latitudes; and (3) the change in areally weighed P_s shows the region where contribution to AM IHO seasonal cycle is larger is at subtropical latitudes.

6 Conclusions and discussion

By use of 1979−2006 NCEP/NCAR reanalysis of daily and monthly surface pressures, meridional winds, radiation and vapor datasets, a study is performed of AM IHO seasonality, achieving that (1) the cycle is pronounced, as is shown in the antiphase feature for both the hemispheres, with the AM IHO seasonal variation linked to the AM redistribution in the whole global domain, and the strongest pressure perturbation contributing most

greatly to the IHO emerges at mid-latitudes; (2) for the AM change, hemispheric vapor mass and cross-equatorial mass flows are the internal factors of the IHO cycle, which exhibit the antiphase seasonal cycle between the hemispheres, with the annual range for hemispheric vapor mass comparable to that in AM, opposite in phase. The interhemispheric air density difference arising from the variation in hemispheric vapor mass results in cross-equatorial mass flow I_1, which evolves in the same phase as the hemispheric AM; (3) the change in hemispheric net surface short- and long-wave radiation is related to the seasonal change of vapor mass and I_1, respectively, suggesting that radiative heating is the dominant external factor of the AM IHO; and (4) the seasonal cycle of globally averaged AM is highly distinct, with its maximum (minimum) occurring in summer (winter) for the boreal hemisphere (and v.v. for the austral hemisphere), with the annual change amount over 10^{15} kg, caused mainly by the variation of global vapor mass, which supports the assumption of the conservation of dry air mass globally from another perspective. Furthermore, the anomalous AM associated with land-sea thermal contrast differs markedly in different seasons, with its zonal (meridional) distribution dominantly in the Northern (Southern) Hemisphere. The IHO seasonal cycle is substantiated in the simulation by CAM3[15] and FrAM1.0[16] with JRA25 and ERA40 employed, arriving at the conclusions consistent broadly with the above.

It should be noted that there are two schemes for calculating cross-equatorial mass flow. The changes in hemispheric AM and vapor mass were used to obtain I_1 in previous papers. Here we present AM transfer I_2 acquired from the vertical integration in the v direction along the equator. Following Guan and Yamagata[10], the AM flow passing the equatorial vertical plane per unit time and unit distance is given as

$$\eta = \frac{1}{2\pi}\int_0^{2\pi}\int_{z_s}^{z_t}(\rho v \mid \varphi = 0)\mathrm{d}z\mathrm{d}\lambda$$
$$= \frac{1}{2\pi g}\int_0^{2\pi}\int_0^{p_s}(v \mid \varphi = 0)\mathrm{d}p\mathrm{d}\lambda\,, \qquad (6)$$

which is the vertical integration form of AM throughout the atmospheric extent, wherein g, λ and φ denote, respectively, the gravitational acceleration, latitude and longitude. In calculation, v is integrated from surface to the data top (10 hPa) and from η we find I_2 on a monthly basis, with the expression of the form:

$$I_2 = \int_0^{ts} 2\pi a\eta \mathrm{d}t, \qquad (7)$$

in which a signifies the earth's radius, and ts the month's length. From the vertical integration of products of layered specific humidities and meridional winds v we acquire cross-equatorial vapor mass transport (I_w). Note that the integration proceeds till the top layer of specific humidity q at 300 hPa.

Figure 6(a) and (b) delineates seasonally-evolving multiyear mean I_2 and I_w. Figure 6(a) shows that in April—November) the AM is transported southwards and over December—March northwards, with the intensity lower than in the former case, exhibiting the thermal properties of hemispheric atmospheric air expanded under the ef- fect of heat, thereby going outwards. In Figure 6(b), the percentage of I_w dominantly at lower levels is smaller compared to that of I_2, with its annual range lower by greater than one order, in an opposite phases to I_2, i.e., vapor mass is carried from the winter into summer hemisphere, a fact consistent with the hemispheric AM change addressed earlier. The Hadley circulation plays an active role in AM transfer at equatorial latitudes in such a way that AM is transported at lower levels from the winter into summer hemisphere and v.v. at

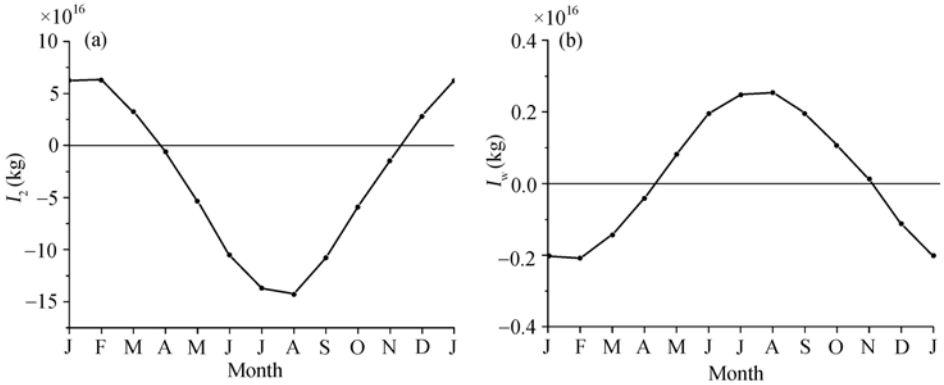

Figure 6 (a) 1979—2006 averaged monthly cross-equatorial AM flow I_2; (b) vapor mass flow I_w.

higher levels, but with higher intensity (figure not shown) into the winter hemisphere, so that as far as the whole atmosphere is concerned the AM is transferred from the summer into winter hemisphere.

At theoretical level, both I_1 and I_2 denote the AM flow through the equator-vertical plane on a monthly basis. It is, however, unfortunate that the calculated yearly range is bigger by ~ one order for I_2 than for I_1, both differing markedly in phase. Graversen et al.[29] made calculation with ERA40 model and related data, maintaining that atmospheric AM change differs significantly from winds-computed meridional AM flow. Allowing for no change in local AM flow hemispherically, the cross-equatorial AM flow is expected to numerically relate to the change in hemispheric AM, i.e., in relation to the air expansion rate on a hemispheric basis. As shown in Figure 1, the change (absolute value) of hemispheric AM is larger in spring and autumn whilst I_2 changes in correspondence to the phase of AM, higher (lower) in winter (summer). The sum of I_2 on a yearly basis arrives at -14.66×10^{16} kg and I_2-derived inter-hemispheric AM transfers annually are not in balance, maybe in association with the poor-quality assimilation data for the v field.

It should be noted that the paper involves just the IHO seasonal variations based on multi-year means. Inspection of Figures 2 and 1 yields that as the principal component for AM change, hemispherically averaged P_w has its interannual variability considerably smaller compared to AM (P_s). Also, Guan and Yamagata[10] demonstrated that interannual vapor variation exerts insignificant impacts on the interannual anomaly in AM for both the hemispheres. These problems await further research in the seasonal features of interannual variability of AM IHO.

The authors would like to thank the Center of Atmospheric Data Service, NUIST under the Geoscience Department of National Natural Science Foundation of China and NOAA-CIRES Climate Diagnostics Center at http://www.cdc.noaa.gov/cdc/reanalysis/reanalysis.shtml for providing data.

1 Toumi R, Hartell N, Bignell K. Mountain station pressure as an indicator of climate change. Geophys Res Lett, 1999, 26: 1751－1754
2 Trenberth K E. Seasonal variations in global sea level pressure and the total mass of the atmosphere. J Geophys Res, 1981, 86: 5238－5246
3 Blewitt G, Lavallee D, Clarke P, et al. A new global mode of earth deformation: Seasonal cycle detected. Science, 2001, 294: 2342－2345
4 Chen T C, Chen J M, Schubert S, et al. Seasonal variation of global surface pressure and water vapor. Tellus, Ser A, 1997, 49: 613－621
5 Hoinka K P. Mean global surface pressure series evaluated from ECMWF reanalysis data. Q J R Meteorol Soc, 1998, 124: 2291－2297
6 Trenberth K E, Smith L. The mass of the atmosphere: A constraint on global analyses. J Clim, 2005, 18: 864－875
7 Zhao Y, Li J P. Discrepancy of mass transport between the northern and southern hemispheres among the ERA-40, NCEP/NCAR, NCEP-DOE AMIP-2, and JRA-25 reanalysis. Geophys Res Lett, 2006, 33: L20817
8 Baldwin M P. Annular modes in global daily surface pressure. Geophys Res Lett, 2001, 28: 4115－4118
9 Jie S M, Bao C L, Hao C J. On the interrelation of sea ice cover between polar regions. Chin Sci Bull (in Chinese), 1995, 40: 632－635
10 Guan Z Y, Yamagata T. Interhemispheric oscillations in the surface air pressure field. Geophys Res Lett, 2001, 28: 263－266
11 Murphree J T, van den Dool H M. Calculating tropical winds from time mean sea level pressure fields. J Atmos Sci, 1988, 45: 3269－3282
12 Kalnay E, Kanamitsu M, Kistler R, et al. The NCEP/NCAR 40-Year Reanalysis Project. Bull Amer Meteorol Soc, 1996, 77: 437－471
13 Onogi K, Tsutsui J, Koide H, et al. The JRA-25 Reanalysis. J Meteor Soc Japan, 2007, 85: 369－432
14 Uppala S M, Kållberg P W, Simmons A J, et al. The ERA-40 re-analysis. Q J R Meteorol Soc, 2005, 131: 2961－3012
15 Collins, and Coauthors. Description of the NCAR Community Atmosphere Model (CAM3). Technical Report NCAR/TN- 464_STR. 2004
16 Guan Z Y, Iizuka S, Chiba M, et al. Frontier Atmospheric General Circulation Model Version 1.0 (FrAM1.0): Model Climatology. Technical Report FTR-1.2000
17 Trenberth K E, Guillemot C J. The total mass of the atmosphere. J Geophys Res, 1994, 99: 23079－23088
18 Yang J C. Inter- monthly variation of mean northern atmospheric mass. Acta Meteor Sin (in Chinese), 1956, 27: 37－59
19 Austin J M. Mechanism of pressure change. In: Malone T F, ed. Compendium of Meteorology. Boston, Massachusetts: American Meteorological Society, 1951. 630－638
20 Chen T C, Yen M C, Pfaendtner J, et al. Annual variation of the global precipitable water and its maintenance; Observation and climate-simulation. Tellus, Ser A, 1996, 49: 1－16
21 van den Dool H, Saha S. Seasonal redistribution and conservation of atmospheric mass in a general circulation model. J Clim, 1993, 6: 22－30
22 Trenberth K E, Christy J, Olson J G. Global atmospheric mass, surface pressure, and water vapor variations. J Geophys Res, 1987, 92: 14815－14826
23 Zeng Q C, Li J P. Bi-hemispheric atmospheric interactions and the essence of monsoon. Chin J Atmos Sci (in Chinese), 2002, 26: 433－448
24 Oort A H. Global Atmospheric Circulation Statistics, 1953－1973. Professional Paper 14. Rockville, MD: NOAA, 1983. 180
25 Saha K, van den Dool H, Saha S. On the annual cycle in surface pressure on the Tibetan Plateau compared to its surroundings. J Clim, 1994, 7: 2014－2019
26 Zhao P, Zhu Y N, Zhang R H. An Asian-Pacific teleconnection in summer troposhperic temperature and accociated Asian climate variability. Clim Dyn, 2007, 29: 293－303
27 Zhao P, Zhang R H, Liu J P, et al. Onset of southwesterly wind over eastern China and associated atmospheric circulation and rainfall. Clim Dyn, 2007, 28: 797－811
28 Chen T C, Baker W E. Global diabatic heating during FGGE SOP-1 and SOP-2. Mon Weather Rev, 1986, 114(12): 2578－2589
29 Graversen R G, Kallen E, Tjernstrom M, et al. Atmospheric mass-transport inconsistencies in the ERA-40 reanalysis. Q J R Meteorol Soc, 2007, 133: 673－680